Magnetization studies of Landau level broadening in two-dimensional electron systems

1996 J. Phys.: Condens. Matter 8 5189

(http://iopscience.iop.org/0953-8984/8/28/004)

J. Phys.: Condens. Matter **8** (1996) 5189–5207. Printed in the UK

Magnetization studies of Landau level broadening in two-dimensional electron systems

A Potts†, R Shepherd†, W G Herrenden-Harker†, M Elliott†, C L Jones‡, A Usher‡, G A C Jones§, D A Ritchie§, E H Linfield§ and M Grimshaw§

† Department of Physics and Astronomy, University of Wales College of Cardiff, PO Box 913, Cardiff CF2 3YB, UK

‡ Department of Physics, Stocker Road, University of Exeter, Exeter EX4 4QL, UK

§ Cavendish Laboratory, Department of Physics, University of Cambridge, Madingley Road, Cambridge CB3 0HE, UK

Received 22 January 1996, in final form 18 April 1996

Abstract. We have used a torque magnetometer to measure de Haas–van Alphen oscillations in the magnetization of two-dimensional electrons in GaAs/AlGaAs heterostructures and multiple-quantum-well systems for temperatures ranging from 0.125 K to 4.2 K and in magnetic fields of up to 15 T. Our results indicate that for high magnetic fields the density of states can be described by a series of Lorentzian-broadened Landau levels with a broadening that is independent of the magnetic field, B, and Landau level index, n. However, at low magnetic fields the Lorentzian-broadened density of states becomes indistinguishable from a Gaussian one with a broadening that is proportional to $B^{1/2}$. The high-field behaviour of the Landau level line-shape is shown to differ appreciably from the low-field case as reported by other workers using both magnetization and other experimental methods. The reliability of this and other experimental techniques is discussed.

1. Introduction

Since the discovery of the integral quantized Hall effect [1] (QHE) the properties of the two-dimensional (2D) electron gas (2DEG) have been extensively studied. The role of the density of states (DOS) is known to be important in influencing many of the phenomena that are associated with the QHE such as edge states [2] and non-local sample resistance [3], as well as being a central feature in any understanding of the fractionally quantized Hall effect [4]. Yet in spite of this there is still no clear consensus regarding the exact form of the Landau level DOS in such systems.

In recent years several attempts have been made to measure Landau level line-shapes and the extent of their broadening using a variety of different experimental techniques. These have included investigations of the specific heat [5, 6], photoluminescence [7], magnetocapacitance [8–12] and magnetization [13–15]. The ideal measurement technique would be one which was capable of directly probing the single-particle DOS but at the same time did not perturb the thermodynamic equilibrium of the system. The greater the perturbation the more difficult it becomes to extract reliable information about the DOS.

Most of the above experimental techniques have significant disadvantages. For example, although photoluminescence is capable of probing the DOS directly by exciting electrons from deep levels, it necessarily perturbs the system in doing so and, in addition, requires a detailed knowledge of optical dispersion in the sample in order to interpret the data.

0953-8984/96/285189+19$19.50

Specific heat measurements are also difficult due to the problems of ensuring adequate thermal isolation of the sample and in measuring the extremely small temperature rises in the 2DEG. There is also the additional problem at low temperatures of ensuring that good thermal coupling exists between the 2DEG, the phonon gas and the resistance thermometer used to measure the temperature rise. The possible existence of a non-thermal phonon distribution, weak phonon–phonon and electron–phonon scattering, and the presence of Kapitza thermal resistances between the sample and the temperature sensor only complicates matters further.

A more popular technique in recent years has been that of magnetocapacitance, due in part to its ease of use; however, its interpretation can be complicated by factors such as coupling of the magnetocapacitance signal to the magnetoresistance of the 2DEG. For example, it is known that Shubnikov–de Haas oscillations in the resistivity of the 2DEG can mimic magnetocapacitance oscillations, and it has recently been shown that the presence of edge states in the 2DEG can also affect the oscillation amplitude [12].

Magnetization measurements of 2D electron systems on the other hand do not suffer from any of the above disadvantages. The measurements are performed using a magnetic field, the same field that quantizes the Landau levels. Consequently, the system itself is unperturbed by the actual measurement process unless the sweep-rate of the field is sufficiently high to cause resistive heating (but this is true of all other experimental methods as well). In addition, because the magnetization is a thermodynamic function it is easily calculated for a given DOS as is shown in section 3. The only significant obstacle in the past to undertaking such measurements has been that of designing apparatus with the required sensitivity. This level of sensitivity is now possible using torque magnetometry.

The need for a magnetization study of Landau level broadening is clear from a study of recent experimental results. To date there is little or no consensus regarding the Landau level line-shape or the magnetic field dependence of the broadening. Various methods have been used to measure both, and a variety of different models for the Landau level DOS have been proposed both theoretically and experimentally. Some workers have reported Gaussian line-shapes [5–9, 11, 13–15], while others claim it is Lorentzian [10]. Some report a broadening parameter, Γ, that is independent [5, 8, 10, 14] of applied magnetic field, B, while others [9, 11, 13, 15] report that Γ varies as $B^{1/2}$. In addition, several authors [5, 7, 9, 11] have resorted to the use of a constant background to the DOS in order to resolve the discrepancy between their experimental results and theory. Other less common variations include a Landau level width that varies with filling factor [7], ν, and a broadening term that is a function of the DOS at the Fermi energy [6], μ. This latter model has been ascribed to weak screening of the charge in the 2DEG. The effect on the broadening of inhomogeneities in the 2D carrier concentration has also been considered [8].

Most of these observations have some basis in theory. Ando and Uemura [16] predicted that short-range potential scattering would result in a broadening that varied as $B^{1/2}$, while theoretical arguments have predicted both elliptical [16] and Gaussian [17] line-shapes for the Landau levels. Recent work [18, 19] has indicated that the broadening, Γ, may undergo a transition from a $B^{1/2}$-dependence at low fields to a broadening that is independent of field as B is increased, the critical parameter being the ratio of the magnetic length, $l_B = (\hbar/eB)^{1/2}$, to the range of the disorder. Other workers [20–22], however, favour a self-consistent screening theory for the 2DEG which results in a broadening that oscillates with field, while Gerhardts and Gudmundsson have attributed the background DOS to sample inhomogeneities [23].

In this paper we shall report the results of magnetization measurements performed on various 2D electron systems. The measurements were performed using a torque

magnetometer similar to those reported previously [13–15], but using much higher magnetic fields and lower temperatures. In this regime the de Haas–van Alphen (dHvA) oscillations display a higher degree of harmonic content which allows them to be compared critically with the various models. We shall show that the broadening of the DOS at large magnetic fields is independent of field and Landau level index, and is Lorentzian in nature with no arbitrary background contribution. This clearly contradicts most of the experimental results presented to date [5–11, 13–15].

2. Experimental arrangement

We have developed a torque magnetometer [15, 24] that is capable of measuring magnetic moments of less than 10^{-12} A m^2 at temperatures down to 80 mK. The magnetometer consists of a gold-coated silicon or gallium arsenide rotor of area 14 mm $\times$ 14 mm which supports the sample under investigation and is suspended by two phosphor-bronze torsion fibres so that it is free to rotate in the magnetic field (see figure 1). Silicon and gallium arsenide were chosen as the materials for the rotor because of their low intrinsic magnetization. When a magnetic field is applied at an angle, θ, to the normal of the sample, a torque is exerted on the sample and rotor due to the anisotropy in the magnetization of the two-dimensional electron gas (it is always perpendicular to the plane of the electron gas), causing the sample and rotor to rotate in the field until an equal and opposite torque is established in the torsion fibres. The angular deflection of the rotor can be detected using two parallel-plate capacitors that are formed by the gold film on the back of the rotor and the two half-leaves of the stator (see figure 1).

By measuring the relative change in capacitance of the two capacitors using a capacitance bridge and lock-in techniques at a frequency of $\sim$10 kHz, the torque on the sample can be determined as a function of magnetic flux density, and hence the magnetization of the sample can be found. The system is calibrated *in situ* using a current-carrying coil of known dimensions supported on the rotor (see figure 1) to generate a known torque. This method appears to be more reliable than the previous one [15] which was to observe the superconducting-to-normal transition of a piece of lead wire.

3. Magnetization of a 2D Fermi system

We have considered two different models for the DOS, $g(E, B)$, each of which assumes a periodic array of Landau levels with the broadening of each level being independent of the Landau level index, n. The first model assumes the broadening to be Gaussian with the DOS given by

$$g(E, B) = \frac{2eB}{h} \frac{1}{\Gamma\sqrt{2\pi}} \sum_{n=-\infty}^{\infty} \exp\left(-\frac{(E - E_n)^2}{2\Gamma^2}\right) \tag{1}$$

where E_n is the energy of the Landau level of index n given by

$$E_n = (n + \tfrac{1}{2})\hbar\omega_c \tag{2}$$

and $\omega_c = eB/m^*$ is the cyclotron frequency. The Landau level broadening, Γ, is assumed to be a function of magnetic field, B, with

$$\Gamma(B) = \Gamma_0 B^p. \tag{3}$$

This is consistent with most theoretical models [16, 18, 19] and experimental observations [5, 7–15] which propose that either $p = 0$ or $p = 1/2$. This assumption will be justified by the experimental results reported in section 4.

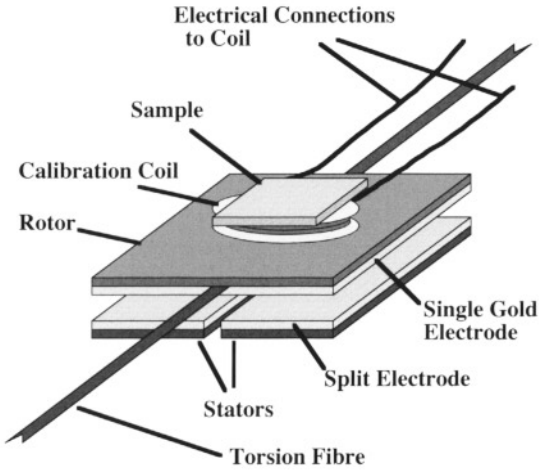

Figure 1. A schematic diagram of the magnetometer and the experimental arrangement used for its calibration with the calibration coil and the sample mounted on the rotor.

The second model that we have considered assumes a Lorentzian-broadened DOS defined by

$$g(E, B) = \frac{2eB}{h}\,\frac{1}{\pi}\sum_{n=-\infty}^{\infty}\frac{\Gamma}{(E-E_n)^2+\Gamma^2}. \tag{4}$$

In recent years several authors have also reported the existence of a constant background to the density of states [5, 7, 9, 11]. This background can be characterized by a parameter ξ representing the magnitude of the background density of states as a fraction of the zero-field density of states. If this is incorporated into our model the modified density of states, $g'(E, B)$, becomes

$$g'(E, B) = \xi\frac{m^*}{\pi\hbar^2} + (1-\xi)g(E, B) \qquad (0 \leqslant \xi < 1). \tag{5}$$

By assuming the Gaussian and Lorentzian DOS models to be periodic *and* symmetric about $E = 0$ it is possible to express them both as Fourier series. Thus, for the Gaussian case, the DOS can be written as

$$g'(E, B) = \frac{m^*}{\pi\hbar^2}\left\{1 + 2(1-\xi)\sum_{s=1}^{\infty}(-1)^s\exp\left(-\frac{2(s\pi\Gamma)^2}{(\hbar\omega_c)^2}\right)\cos\left(\frac{2s\pi E}{\hbar\omega_c}\right)\right\} \tag{6}$$

while for the Lorentzian broadening it becomes

$$g'(E, B) = \frac{m^*}{\pi\hbar^2}\left\{1 + 2(1-\xi)\sum_{s=1}^{\infty}(-1)^s\exp\left(-\frac{2s\pi\Gamma}{\hbar\omega_c}\right)\cos\left(\frac{2s\pi E}{\hbar\omega_c}\right)\right\}. \tag{7}$$

In both cases the background DOS parameter ξ has been included and it can be seen that its effect is to reduce the amplitude of the oscillations by a factor of $(1-\xi)$.

In order to analyse our experimental data we have developed an analytical model for the magnetization that is an extension of that proposed by Shoenberg [25], but extended to include Landau level broadening and the effect of a background DOS. The starting point

for this model is the grand thermodynamic potential per unit area, $\Omega(B)$, from which the 2D magnetization is derived according to equation (8):

$$M(B) = -\left(\frac{\partial \Omega}{\partial B}\right)_{T,\mu}. \tag{8}$$

It has been shown by Shoenberg [25] that if the DOS is periodic, it is possible to derive analytical expressions for the carrier density, n_s, and grand thermodynamic potential, $\Omega(B)$, using the Fourier series expressions for the DOS described in equations (6) and (7). These expressions for n_s and $\Omega(B)$ will hold for any 2D electron system for which the condition $\mu \gg kT$ is satisfied.

The grand thermodynamic potential can be evaluated using the expression

$$\Omega(B) = kT \int_0^\infty g'(E, B) \ln\left[1 - f(E, \mu)\right] \, \mathrm{d}E \tag{9}$$

where $f(E, \mu)$ is the Fermi function given by

$$f(E, \mu) = \frac{1}{1 + \exp((E - \mu)/kT)}. \tag{10}$$

For the case of Gaussian broadening equation (9) can be rewritten as

$$\Omega(B) = \frac{m^* kT}{\pi \overline{h}^2} \left\{ I_3 + 2(1 - \xi) \sum_{s=1}^{\infty} (-1)^s \exp\left(-\frac{2(s\pi\Gamma)^2}{(\overline{h}\omega_c)^2}\right) I_4 \right\} \tag{11}$$

where

$$I_3 = \int_0^\infty \ln\left[1 - f(E, \mu)\right] \, \mathrm{d}E = -\left\{ \frac{\mu^2}{2kT} + \frac{\pi^2 kT}{6} \right\} \tag{12}$$

and

$$I_4 = \int_0^\infty \ln\left[1 - f(E, \mu)\right] \cos\left(\frac{2\pi s E}{\overline{h}\omega_c}\right) \, \mathrm{d}E = -\frac{(\overline{h}\omega_c)^2}{4\pi^2 s^2 kT} + \frac{\overline{h}\omega_c}{2s} \frac{\cos(2\pi s\mu/\overline{h}\omega_c)}{\sinh(2\pi^2 skT/\overline{h}\omega_c)} \tag{13}$$

while for Lorentzian broadening equation (9) becomes

$$\Omega(B) = \frac{m^* kT}{\pi \overline{h}^2} \left\{ I_3 + 2(1 - \xi) \sum_{s=1}^{\infty} (-1)^s \exp\left(-\frac{2s\pi\Gamma}{\overline{h}\omega_c}\right) I_4 \right\}. \tag{14}$$

Because the magnetization measurement is a contactless measurement, the 2D electron carrier density remains constant as the magnetic field is varied, and it is the chemical potential, μ, that oscillates with the magnetic field. Therefore, in order to evaluate the 2D magnetization, $M(B)$, it is necessary to determine $\mu(B)$ for each value of B. This is done using a bisection method subject to the constraint of particle conservation:

$$n_s = \int_0^\infty f(E, \mu) g'(E, B) \, \mathrm{d}E. \tag{15}$$

Using the same method of integration for n_s as for the grand potential above, and again requiring that $\mu \gg kT$, equation (15) can be rewritten as

$$n_s = \frac{m^*}{\pi \overline{h}^2} \left\{ I_1 + 2(1 - \xi) \sum_{s=1}^{\infty} (-1)^s \exp\left(-\frac{2(s\pi\Gamma)^2}{(\overline{h}\omega_c)^2}\right) I_2 \right\} \tag{16}$$

for Gaussian broadening and

$$n_s = \frac{m^*}{\pi\hbar^2}\left\{I_1 + 2(1-\xi)\sum_{s=1}^{\infty}(-1)^s \exp\left(-\frac{2s\pi\Gamma}{\hbar\omega_c}\right) I_2\right\} \tag{17}$$

for Lorentzian broadening where I_1 is given by

$$I_1 = \int_0^{\infty} f(E,\mu)\ \mathrm{d}E = \mu + kT\ln(1+\mathrm{e}^{-\mu/kT}) \tag{18}$$

and I_2 by

$$I_2 = \int_0^{\infty} f(E,\mu)\cos\left(\frac{2\pi sE}{\hbar\omega_c}\right)\mathrm{d}E = \pi kT\frac{\sin(2\pi s\mu/\hbar\omega_c)}{\sinh(2\pi^2 skT/\hbar\omega_c)}. \tag{19}$$

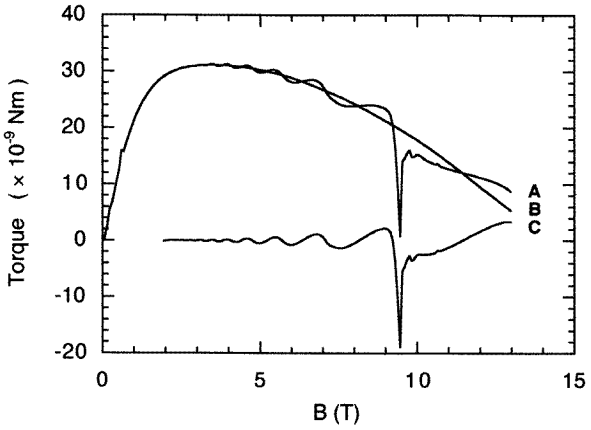

Figure 2. The magnetometer output at a temperature of 0.3 K in terms of torque as a function of external magnetic flux for the ten-period GaAs/AlGaAs multiple-quantum-well sample. The original data are shown as curve A, while curve B represents the best fit to the background due to the rotor and the sample substrate. The difference between the two curves (curve C) is ascribed to the contribution of the two-dimensional electrons to the torque. The peaks at $B = 9.45$ T are due to eddy currents.

From equations (8) and (11)–(14) it is possible to derive expressions for the 2D magnetization, $M(B)$. For the case of Gaussian broadening this is found to be

$$M(B) = -(1-\xi)\frac{2m^*kT}{\pi\hbar^2}\sum_{s=1}^{\infty}(-1)^s\exp\left(-\frac{2[\pi s\Gamma(B)]^2}{(\hbar\omega_c)^2}\right)\left[\left(\frac{\partial I_4}{\partial B}\right)_{\mu,T} + (1-p)\left[\frac{2\pi s\Gamma(B)}{\hbar\omega_c}\right]^2\frac{I_4}{B}\right] \tag{20}$$

and for Lorentzian broadening

$$M(B) = -(1-\xi)\frac{2m^*kT}{\pi\hbar^2}\sum_{s=1}^{\infty}(-1)^s\exp\left(-\frac{2\pi s\Gamma(B)}{\hbar\omega_c}\right) \times \left[\left(\frac{\partial I_4}{\partial B}\right)_{\mu,T} + (1-p)\frac{2\pi s\Gamma(B)}{B\hbar\omega_c}I_4\right] \tag{21}$$

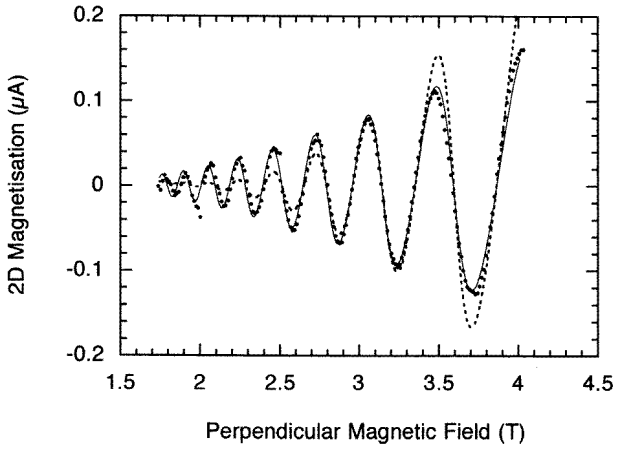

Figure 3. 2D magnetization (solid dots) versus perpendicular magnetic flux density, B, for the ten-period GaAs/AlGaAs multiple-quantum-well structure at a temperature of 1.2 K together with the best fits to the data assuming a Gaussian broadening of the Landau levels and two models for the broadening of $\Gamma = 1.92$ meV (dashed curve) and $\Gamma = 1.09\sqrt{B}$ meV (solid curve). For clarity only one data point in five is shown.

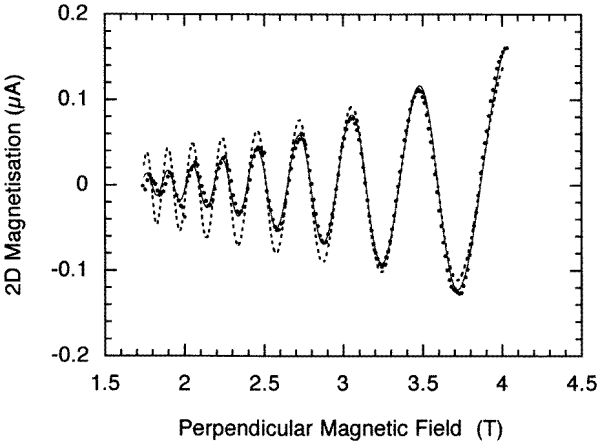

Figure 4. 2D magnetization (solid dots) versus perpendicular magnetic flux density, B, for the ten-period GaAs/AlGaAs multiple-quantum-well structure at a temperature of 1.2 K together with the best fits to the data assuming a Lorentzian broadening of the Landau levels and two models for the broadening of $\Gamma = 2.16$ meV (solid curve) and $\Gamma = 1.16\sqrt{B}$ meV (dashed curve). For clarity only one data point in five is shown.

where

$$\left(\frac{\partial I_4}{\partial B}\right)_{\mu,T} = \frac{1}{B}\left\{-\frac{(\hbar\omega_c)^2}{2\pi^2 s^2 kT} + \pi\mu\frac{\sin(2\pi s\mu/\hbar\omega_c)}{\sinh(2\pi^2 skT/\hbar\omega_c)} + \frac{\cos(2\pi s\mu/\hbar\omega_c)}{\sinh(2\pi^2 skT/\hbar\omega_c)}\left[\frac{\hbar\omega_c}{2s} + \pi^2 kT\coth\left(\frac{2\pi^2 skT}{\hbar\omega_c}\right)\right]\right\}. \tag{22}$$

The term p in equations (20) and (21) is the B-field dependence of Γ (see equation (3)).

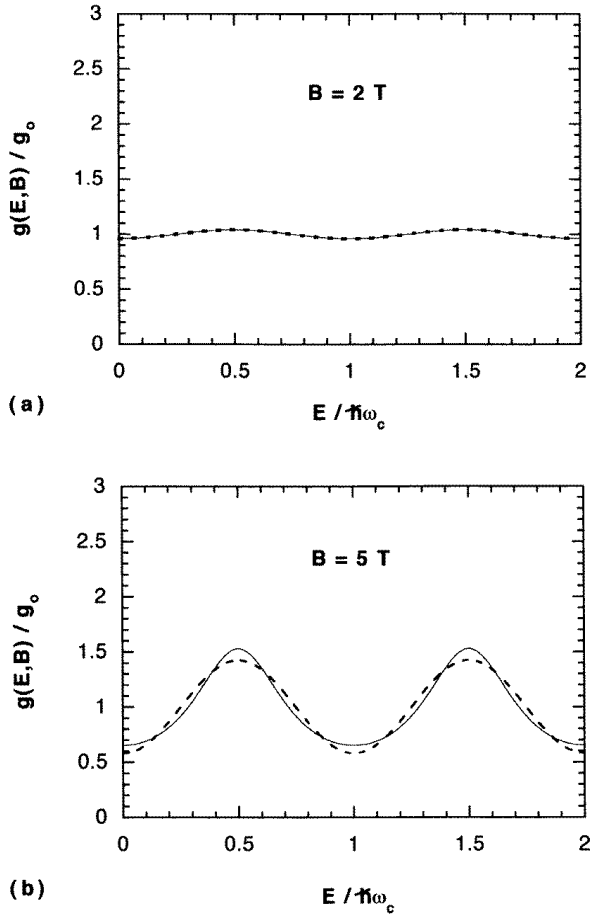

Figure 5. The density of states $g(E, B)$ of a 2DEG in GaAs as a function of electron energy E and magnetic field B for Lorentzian-broadened Landau levels with $\Gamma = 2.16$ meV (solid curve) and Gaussian-broadened levels with $\Gamma = 1.09\sqrt{B}$ meV (dashed curve) for four different magnetic flux densities: (a) $B = 2$ T, (b) $B = 5$ T, (c) $B = 8$ T and (d) $B = 11$ T. The ordinate and abscissa axes are normalized in units of $g_0 = m^*/\pi\hbar^2$ and $\hbar\omega_c$ respectively.

The above analysis is conditional on the inequality $\mu \gg kT$ being satisfied. While this will be true for measurements made on a system with a high carrier density and low effective mass at low temperatures it will not always be so, for while the expression for I_1 is exact, those for I_2, I_3 and I_4 are merely approximations, their relative error being determined by the parameter $\Delta = \exp(-\mu/kT)$. For the samples described in this paper $\Delta < 10^{-25}$ at $T = 4.2$ K and so any corrections to the terms I_2, I_3 and I_4 can be disregarded. It should be pointed out, however, that for samples of fixed carrier density n_s, the expressions for the grand potential, $\Omega(B)$, and the 2D magnetization, $M(B)$, are extremely sensitive functions of the chemical potential, $\mu(B)$, and so great care is needed in the numerical determination of $\mu(B)$ from equation (16) or (17). For this reason the correction terms to I_2, I_3 and I_4 are given in the appendix for future reference.

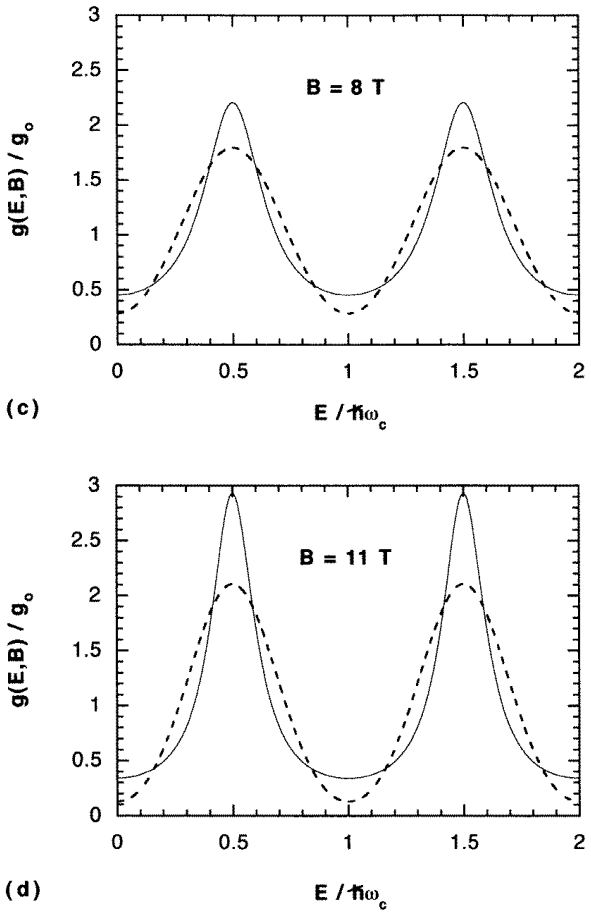

Figure 5. (Continued)

4. Experimental results

We have used the analytical expressions for $M(B)$ (equations (13) and (20)–(22)) to analyse the magnetization of a ten-period GaAs/AlGaAs multiple-quantum-well structure. The structure was grown by MBE on a semi-insulating GaAs substrate, and Shubnikov–de Haas and Hall measurements indicated that the carrier density per layer, n_s, was 1.2×10^{16} m^{-2} at 4.2 K while the Hall mobility was 2.9 m^2 V^{-1} s^{-1}. These results equate to a transport lifetime, τ, of 1.1 ps and an elastic mean free path of 0.5 μm. The width of the GaAs potential wells is 10 nm and their periodicity is 47 nm.

The magnetization of a 14 mm $\times$ 14.5 mm slice of the multiple-quantum-well sample was measured using the magnetometer and experimental arrangement shown in figure 1 at a temperature of 1.2 K. During the measurement the sample was oriented with its normal at an angle of 30° to the magnetic field direction while the field was swept up from zero. Figure 2 shows a typical plot of the resulting torque on the sample as a function of the total external magnetic flux density. It can be seen that in addition to the oscillations there is a large paramagnetic background signal at low fields (which we assume is due to impurities in

the rotor) and a large eddy current peak at $B = 9.45$ T. Initial magnetization measurements were made using an n^- silicon rotor; however, we have recently found that semi-insulating GaAs gives a much lower background signal which we attribute to its much lower impurity concentration.

The background signal was removed from the raw data (curve A in figure 2) using a fitting routine and a trial algebraic function (curve B) to give the torque due to the 2DEG (curve C). The actual magnetization of the 2DEG is then derived from curve C by dividing the data by $BAN\sin\theta$ where A is the area of the sample and N is the number of 2D layers (in this case $N = 10$).

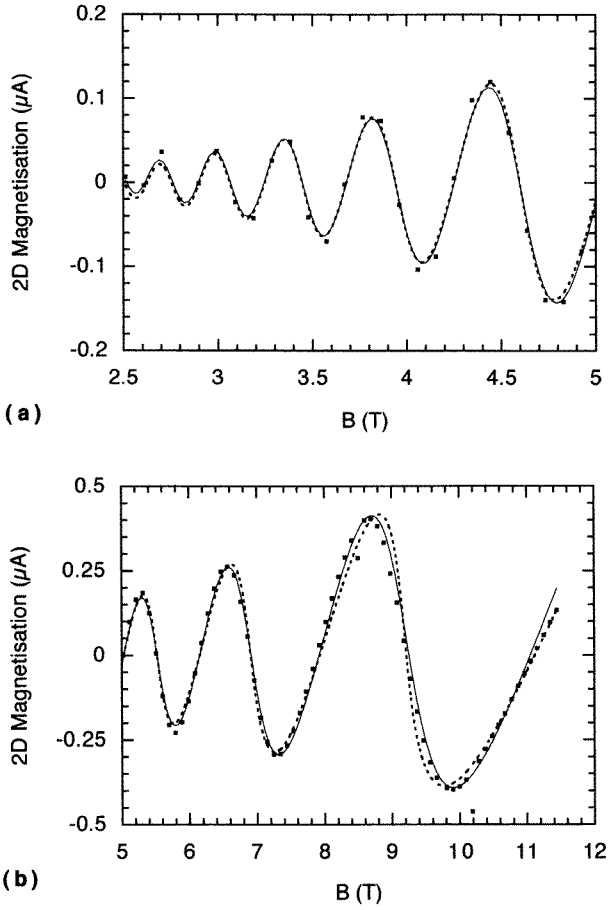

Figure 6. 2D magnetization (solid squares) of the ten-period GaAs/AlGaAs multiple-quantum-well sample at $T = 4.2$ K together with the best fits to the data for a Lorentzian DOS with a broadening of $\Gamma = 2.675$ meV (solid curve) and a Gaussian DOS with a broadening of $\Gamma = 1.212\sqrt{B}$ meV (dashed curve). B is the perpendicular magnetic flux density. For clarity the (a) low-field and (b) high-field data are shown separately.

When comparing the experimental magnetization data with theory we have considered two different models for the Landau level line-shape: Lorentzian and Gaussian; and two different models for the broadening: constant Γ and $\Gamma \propto \sqrt{B}$. These models are shown, together with the experimental data, in figure 3 and figure 4. In fitting to the experimental

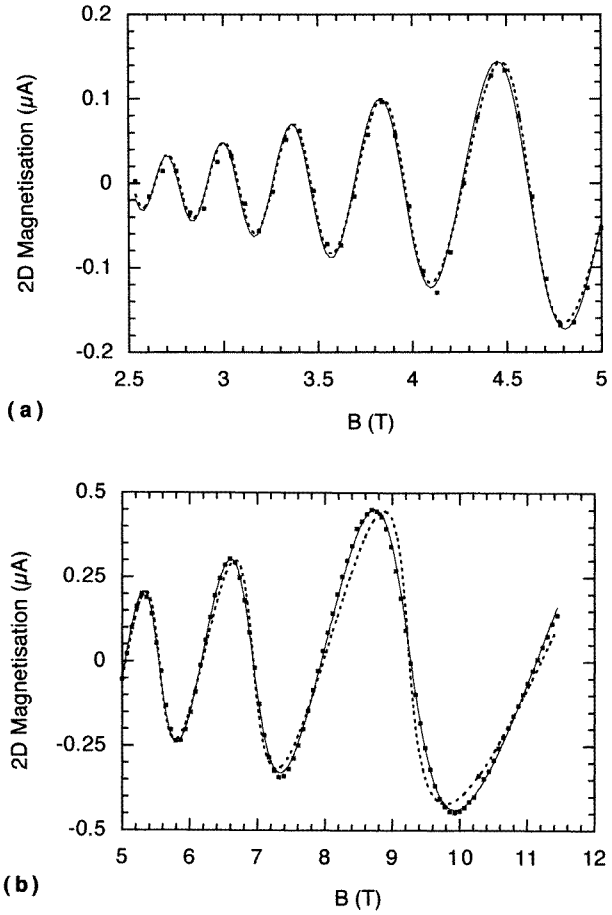

Figure 7. 2D magnetization (solid squares) of the ten-period GaAs/AlGaAs multiple-quantum-well sample at $T = 2.2$ K together with the best fits to the data for a Lorentzian DOS with a broadening of $\Gamma = 2.529$ meV (solid curve) and a Gaussian DOS with a broadening of $\Gamma = 1.189\sqrt{B}$ meV (dashed curve). B is the perpendicular magnetic flux density. For clarity the (a) low-field and (b) high-field data are shown separately.

data only two fitting parameters were initially employed, the carrier density, n_s, and the Landau level broadening, Γ_0. The background DOS as characterized by the parameter ξ was assumed to be zero. No spin splitting was observed in any of the samples discussed here and so was not included in any of the theoretical models.

It can be seen from figure 3 that for Gaussian broadening the $\Gamma \propto \sqrt{B}$ model fits the data much better than the constant-broadening case, while figure 4 indicates that for Lorentzian broadening the reverse is true. A comparison of figure 3 with figure 4 indicates that over this particular field range ($2\ \text{T} < B < 5\ \text{T}$) there is no significant difference between the Lorentzian model with constant broadening ($\Gamma = 2.16$ meV) and the Gaussian model with $\Gamma = 1.09\sqrt{B}$ meV. This is not particularly surprising since equations (6) and (7) indicate that the fundamental frequency components ($s = 1$) of the DOS in each case are virtually identical and at low fields the contribution of the harmonics ($s > 1$) will be negligible. This is further illustrated in figure 5 which shows the DOS as a function of

energy for the two theoretical models in question (equations (6) and (7)). It is clear that at low fields the DOS described by the two models are indistinguishable and only at high fields is there an appreciable difference.

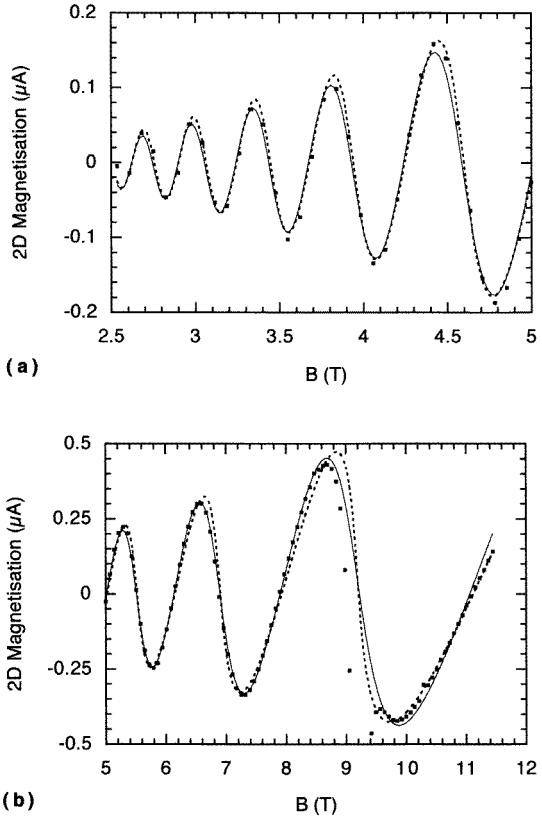

Figure 8. 2D magnetization (solid squares) of the ten-period GaAs/AlGaAs multiple-quantum-well sample at $T = 0.55$ K together with the best fits to the data for a Lorentzian DOS with a broadening of $\Gamma = 2.522$ meV (solid curve) and a Gaussian DOS with a broadening of $\Gamma = 1.165\sqrt{B}$ meV (dashed curve). B is the perpendicular magnetic flux density. For clarity the (a) low-field and (b) high-field data are shown separately. Note also the deviation between the data and the two models for 8.5 T $< B <$ 9.5 T due to the presence of an eddy current peak.

Further measurements were made in fields of up to 15 T over a range of temperatures between 0.125 K and 4.2 K with the sample immersed in the dilute phase of a ^{3}He/^{4}He dilution refrigerator. The sample was tilted so that the normal to the 2DEG was aligned at an angle of 15° to the field. For these measurements a different magnetometer design was employed in which the split electrode on the stator was suspended on a second rotor of identical size to that supporting the sample [24]. In this way the background signal due to the paramagnetic moment of the sample-carrying rotor could be significantly reduced. Unfortunately, this experimental arrangement precluded any direct *in situ* calibration of the magnetometer sensitivity. Calibration was therefore performed by comparing the amplitudes of the dHvA oscillations below 5 T with those observed previously for the same sample at the same temperature in a calibrated run.

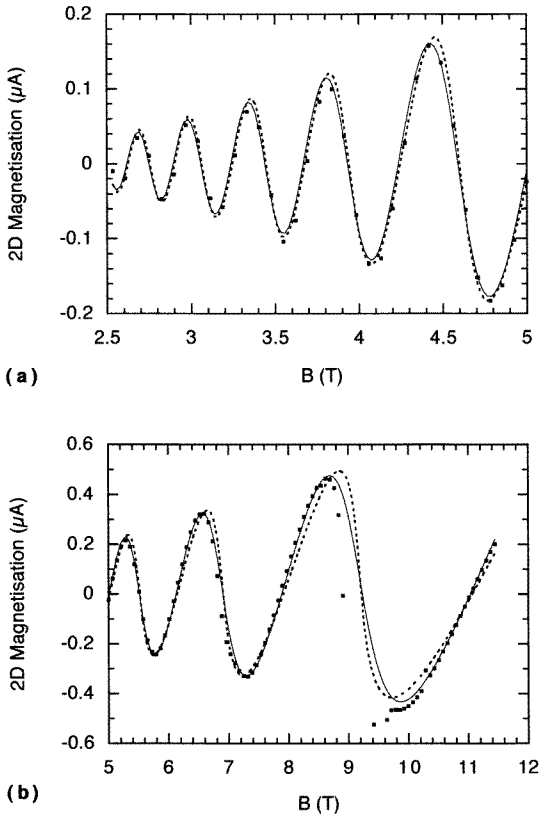

Figure 9. 2D magnetization (solid squares) of the ten-period GaAs/AlGaAs multiple-quantum-well sample at $T = 0.3$ K together with the best fits to the data for a Lorentzian DOS with a broadening of $\Gamma = 2.469$ meV (solid curve) and a Gaussian DOS with a broadening of $\Gamma = 1.157\sqrt{B}$ meV (dashed curve). B is the perpendicular magnetic flux density. For clarity the (a) low-field and (b) high-field data are shown separately. Note also the deviation between the data and the two models for 8.7 T $< B <$ 9.7 T due to the presence of an eddy current peak.

Figure 6 shows a typical set of data at 4.2 K together with two theoretical fits, one due to a Lorentzian DOS with constant broadening and the other due to a Gaussian DOS with $\Gamma \propto \sqrt{B}$. For clarity the low-field and high-field data in figure 6 are shown in separate figures (figure 6(a) and figure 6(b)). It can be seen that at low fields the data are consistent with those shown in figure 3 and figure 4, with both models for the DOS resulting in equally convincing fits to the magnetization data. However, at the highest fields there is a significant difference between the two models, particularly in the characteristic shape of the oscillations that each model describes. The Gaussian DOS with $\Gamma \propto \sqrt{B}$ results in oscillations that are more saw-tooth in character, possessing a greater harmonic content. The Lorentzian DOS with constant broadening, on the other hand, results in oscillations which are more sinusoidal and show better agreement with the experimental data. This behaviour was repeated at every temperature investigated with the Lorentzian model always proving a significantly better fit to the data. This can be seen from the data in figure 7, figure 8 and figure 9 which were measured at $T = 2.2$ K, $T = 0.55$ K and $T = 0.3$ K

respectively.

It can also be seen from figures 8 and 9 that at temperatures below 1.0 K eddy current peaks begin to be observed at integer filling factors. These arise as a consequence of the zero-resistance phase associated with the localized states between Landau levels and are only observed when the overlap of the tails of adjacent Landau levels is such that all of the states in the mid-gap are localized. In this particular sample, however, the absence of any significant spin-splitting of the Landau levels means that only even-numbered filling factors are observed. The eddy current peaks seen at $B = 9.15$ T in figures 8 and 9 occur for filling factors of $\nu = 6$ (or a Landau level index $n = 3$), though peaks at $B = 6.9$ T corresponding to $\nu = 8$ were observed at lower temperatures.

The magnitude of the eddy current peaks depends on the sweep rate of the magnetic field and can result in magnetic moments many times greater than the amplitude of the dHvA oscillations (see figure 2). Such large peaks tend to obscure the underlying dHvA oscillations. Consequently all data points in the vicinity of eddy current peaks were excluded from the fitting procedure in order that they would not distort the results. In addition, no fitting to data above $B = 11.5$ T was attempted because of uncertainty in the position of the background in the region of the last oscillation due to the divergence in oscillation amplitude with field. The eddy currents themselves are extremely long-lived due to the dissipationless state of the quantum Hall plateaux. Their characteristic decay time as a function of temperature and Landau level index has already been investigated [24] and has been found to exceed several hours in duration.

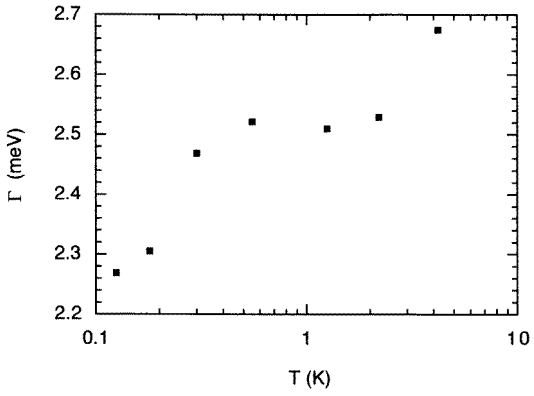

Figure 10. The temperature dependence of the Landau level broadening, Γ, assuming a Lorentzian-broadened density of states (solid squares).

The magnetization of the multiple-quantum-well sample was measured at seven different temperatures between 0.125 K and 4.2 K. The results of the fitting procedure indicated that the Landau level broadening has a small but significant positive temperature dependence (see figure 10). Such behaviour is not inconsistent with that observed for the electron mobility in GaAs/AlGaAs heterostructures where the temperature-dependent term is thought to arise from scattering by acoustic phonons [26]. Unfortunately, the scatter in the data points in figure 10 precludes any detailed analysis of the temperature dependence of Γ in this case.

The above fits all assume the background DOS to be negligible. To test this hypothesis the above data were refitted with a background DOS as characterized by the fitting parameter ξ included in addition to the previous fitting parameters, n_s and Γ. The results of this procedure indicated that for the low-field data in figure 3 and figure 4 the inclusion of a

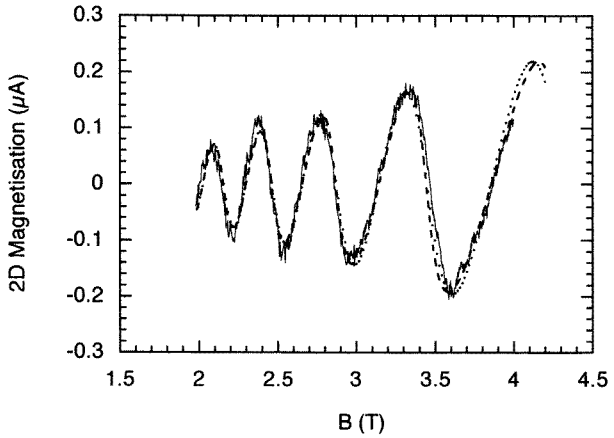

Figure 11. 2D magnetization (solid curve) versus the perpendicular magnetic flux density, B, for sample 1-1107A at a temperature of 1.2 K. The 2D carrier concentration is 8.31×10^{15} m^{-2} and the 77 K mobility is 4.7 m^2 V^{-1} s^{-1}. Also shown are the two best fits to the data, one employing a Lorentzian broadening of $\Gamma = 1.34$ meV (dotted curve) and the other a Gaussian broadening of $\Gamma = 0.862\sqrt{B}$ meV (dashed curve).

background DOS resulted in values for ξ that were less than 0.04 for both the Lorentzian-broadened DOS model with a magnetic-field-independent Γ, and the Gaussian-broadened DOS model with $\Gamma \propto B^{1/2}$. For the high-field data (figures 6 to 9) the outcome was similar with ξ always less than 0.04 except at the highest temperature investigated ($T = 4.2$ K) where it rose to 0.08. We attribute this rise to the increased experimental error at high temperatures due to the reduced amplitude of the oscillations. The values obtained for ξ are significantly less than the contribution that the broadening makes to the DOS between Landau levels (see figure 5). This would appear to indicate that the DOS between Landau levels in this sample can be accounted for entirely by the broadening of the levels themselves without the need to resort to an *ad hoc* background term.

In addition to a ten-period multiple-quantum-well sample we have also measured the magnetization at 1.2 K of several single-layer GaAs/AlGaAs heterostructure samples with mobilities between 1.5 m^2 V^{-1} s^{-1} and 5.0 m^2 V^{-1} s^{-1} using fields of up to 5 T. Because these samples have only one 2DEG, the dHvA signal is significantly reduced in comparison with that of the ten-layer sample, and the effects of mechanical vibration and the background magnetization of the rotor become more significant. Nevertheless, in spite of these difficulties, these samples clearly show the same qualitative results for the broadening as the multiple-quantum-well sample over the same field range. The magnetization data for a typical sample are shown in figure 11 (sample 1-1107A). In this and all other similar samples with mobilities of up to 5.0 m^2 V^{-1} s^{-1} that we have so far investigated, the Gaussian $B^{1/2}$ DOS model and constant-broadening Lorentzian DOS model prove to be equally convincing fits to the data at low magnetic fields and, as for the multiple-quantum-well sample, are virtually indistinguishable.

5. Discussion

The results presented here clearly differ from most of those that have been reported previously using both magnetization [13–15] and other experimental techniques [5–9, 11].

One reason for this may be the relative sensitivity of the various experimental procedures used. It can be seen from figures 6–9 and figure 11 that the difference between the Gaussian $B^{1/2}$ and constant-broadening Lorentzian models is small and would be difficult to detect in lower-mobility samples or at lower fields and higher temperatures. Indeed, it is clear that this difference is much smaller than the disparity in the single-particle DOS for the two models. This will be true for all thermodynamic potentials and any quantity that depends on the thermodynamic DOS, and is therefore a problem that will also be encountered in magnetocapacitance and heat capacity measurements. The reason for this can be found in the temperature-dependent $x/\sinh(x)$ term of the thermodynamic DOS which increases the damping of the higher-harmonic terms. Yet it is these harmonics that allow the two models to be distinguished. Thus, the greater this damping term becomes (i.e. at high temperatures and low magnetic fields), the harder it is to distinguish between the Gaussian $B^{1/2}$ and constant-broadening Lorentzian models. This could partially explain why the constant-broadening Lorentzian model has not been reported previously.

Despite this however, it is clear that no consensus yet exists regarding the exact form of the Landau level DOS in 2D systems. The fact that so many different techniques yield so many different results for the DOS suggests that at least some of these results owe more to the actual experimental method employed than to the nature of the system under investigation. With the exception of magnetization, most experimental determinations of the DOS involve perturbing the system. As a result, in some cases it is often not entirely clear what it is that is actually being measured or how reliable those measurements may be. This does not mean that such techniques are of no practical use (although some do appear to require a greater leap of faith than others), merely that they require corroboration. Magnetization can provide such corroboration, yet until recently very little work has been reported using this technique.

Previous magnetization measurements [13–15] have yielded results which at first sight appear to differ slightly from those presented here. The difference between the Gaussian $B^{1/2}$-model observed in previous work [13, 15] and the constant-broadening Lorentzian model observed here may be explained in part by the greater sensitivity, temperature and field range of our magnetometer system which allows these differences to be observed more clearly than has been possible previously. In addition, our *in situ* calibration results in more accurate data which also show closer agreement with theory than previous experimental data. It should also be noted that some previous results [14] involved the filtering of data, a procedure which could result in the removal of the harmonic components which help to distinguish between the different DOS models.

Our results for the magnetic field dependence of the broadening are, however, consistent with recent theoretical work [18, 19] which suggests that at low fields the Landau level width, Γ, should vary with magnetic field as $\Gamma \propto \sqrt{B}$, whereas at high fields it should be independent of field. The critical parameter in determining which model should be applicable is the ratio of the magnetic length, l_B, to the extent of the disorder (the correlation length).

The quality of the fits that we obtain also negates the need to introduce the concept of a background DOS. This may be due to the fact that the extent of the broadening in our samples ensures that even at the highest fields ($B \sim 11$ T) there remains a significant DOS between Landau levels. This can be as high as 33% of the zero-field value due to the comparatively slow decay ($\sim E^{-2}$) of the Lorentzian line-shape when compared with its Gaussian counterpart. In addition, we see no evidence to support the theory that the broadening oscillates with field due to changes in electron screening as has been advocated by some workers [6].

The results that we have presented here are also similar to those of Ashoori and Silsbee [10] who claim to have observed Lorentzian broadening of Landau levels in magnetocapacitance measurements of a double-barrier tunnelling structure with the broadening Γ being independent of B. However, they also reported that the broadening increased with decreasing filling factor, $\nu = eB/h$, particularly where the filling factor approached the quantum limit (where $\nu \sim 1$). This feature of their results could be a consequence of their experimental method which involved measuring the magnetocapacitance at a constant magnetic field while varying the gate bias which controlled the chemical potential (and hence the carrier concentration n_s) in the potential well. Hence by adjusting the bias to reduce the filling factor they would necessarily reduce the carrier concentration in the well. This would in turn reduce the amount of screening and therefore increase the broadening of the Landau levels. In our measurements, by contrast, n_s is kept constant and so any changes in screening will be less significant. This could explain why we have found no evidence for a filling factor dependence of the broadening in any of our samples, although so far we have restricted our measurements to the case where $\nu \geqslant 6$.

So far our work has been confined to comparatively low-mobility samples (<5.0 m^2 V^{-1} s^{-1}) with relatively high 2D carrier densities, where the Landau level broadening is comparatively large and does not appear to be significantly influenced by the theoretically predicted variation in electron screening [22]. In order to finally resolve the issue of Landau level line-shape it would be desirable to extend this work to samples of higher mobility. Such samples generally exhibit a reduced Landau level broadening that would allow the differences in the various theoretical DOS models to become more apparent. Unfortunately they would also have a smaller carrier density than those investigated here, and this in turn would reduce the amplitude of the oscillations, while their increased mobility may make them more susceptible to induced eddy currents upon sweeping the field [24].

6. Summary

We have presented results of a systematic study of the magnetization of 2D electron systems in the quantum Hall regime that indicate that at high magnetic fields the DOS consists of a periodic array of Lorentzian-broadened Landau levels with the broadening being independent of the magnetic field and Landau level index. These results clearly show a different behaviour of the magnetization of 2D electron systems from those previously reported at lower fields [13–15]. This, we believe, is due to the greater sensitivity and low-temperature capability of our magnetometer, and our improved background removal and calibration procedure. These results also differ considerably from those determined using other experimental techniques such as photoluminescence, specific heat and magnetocapacitance. We attribute this to the non-equilibrium nature of those experimental methods which are all known to perturb the system under investigation to some degree and which are more difficult to model accurately than the magnetization method.

Acknowledgments

The work at Cardiff and Exeter was supported by a grant from the EPSRC. In addition, the authors would like to thank Epitaxial Products International Ltd (Cardiff) for supplying some of the single-heterostructure samples.

Appendix

The equations for I_2, I_3 and I_4 (equations (19), (12) and (13) respectively) are approximations that apply in the limit of low temperature and high chemical potential, μ. However, it is possible to extend these equations to any degree of accuracy in the following manner.

The equations for I_2 and I_4 are derived using the identity [25]

$$\int_{-\infty}^{\infty} \frac{e^{iax}}{2\,[1+\cosh(x)]}\,dx = \frac{\pi a}{\sinh(\pi a)}. \tag{A1}$$

The integral expression for I_2

$$I_2 = \int_0^{\infty} f(E,\mu)\cos\left(\frac{2s\pi E}{\hbar\omega_c}\right) dE \tag{A2}$$

can be integrated by parts to give

$$I_2 = \frac{\hbar\omega_c}{4s\pi kT}\int_0^{\infty} \frac{1}{1+\cosh((E-\mu)/kT)}\sin\left(\frac{2s\pi E}{\hbar\omega_c}\right) dE \tag{A3}$$

and this may be rewritten as

$$I_2 = \pi kT\frac{\sin(2\pi s\mu/\hbar\omega_c)}{\sinh(2\pi^2 skT/\hbar\omega_c)} - \frac{\hbar\omega_c}{4s\pi\ kT}\int_{-\infty}^{0} \frac{\sin(2s\pi E/\hbar\omega_c)}{1+\cosh((E-\mu)/kT)}\,dE. \tag{A4}$$

The final integral is the correction term and it can be evaluated by rewriting the $1/(1+\cosh(x))$ term where $x = (E-\mu)/kT$ as a power series in e^x and integrating each term separately. The expression for I_2 then becomes

$$I_2 = \pi kT\frac{\sin(2\pi s\mu/\hbar\omega_c)}{\sinh(2\pi^2 skT/\hbar\omega_c)} - kT\sum_{n=1}^{\infty}(-1)^n \frac{n}{n^2+(2\pi^2 skT/\hbar\omega_c)^2} e^{-n\mu/kT}. \tag{A5}$$

The main application of this expression is when the carrier density, n_s, needs to be calculated extremely accurately in order to determine $\mu(B)$ precisely. Fortunately, because of the exponential term, the summation converges extremely rapidly.

Comparable results can be derived for I_3 and I_4 using a similar method and will yield the following expressions:

$$I_3 = -\left\{\frac{\mu^2}{2kT} + \frac{\pi^2 kT}{6} + kT\sum_{n=1}^{\infty}\frac{(-1)^n}{n^2}\ e^{-n\mu/kT}\right\} \tag{A6}$$

and

$$I_4 = -\frac{(\hbar\omega_c)^2}{4\pi^2 s^2 kT} + \frac{\hbar\omega_c}{2s}\frac{\cos(2\pi s\mu/\hbar\omega_c)}{\sinh(2\pi^2 skT/\hbar\omega_c)} - kT\sum_{n=1}^{\infty}(-1)^n\frac{e^{-n\mu/kT}}{n^2+(2\pi^2 skT/\hbar\omega_c)^2}. \tag{A7}$$

References

[1] von Klitzing K, Dorda G and Pepper M 1980 *Phys. Rev. Lett.* **45** 494
[2] van Haren R J F, Blom F A P and Wolter J H 1995 *Phys. Rev. Lett.* **74** 1198
[3] Büttiker M, Imry Y, Landauer R and Pinhas S 1985 *Phys. Rev.* B **31** 6207
[4] Tsui D C, Stormer H L and Gossard A C 1982 *Phys. Rev. Lett.* **48** 1559
[5] Gornik E, Lassnig R, Strasser G, Stormer H L, Gossard A C and Wiegmann W 1985 *Phys. Rev. Lett.* **54** 1820
[6] Wang J K, Campbell J H, Tsui D C and Cho A Y 1988 *Phys. Rev.* B **38** 6174
[7] Berendschot T T J M, Reinen H A J M and Bluyssen H J A 1987 *Solid State Commun.* **63** 873
[8] Smith T P, Goldberg B B, Stiles P J and Heiblum M 1985 *Phys. Rev.* B **32** 2696
[9] Mosser V, Weiss D, von Klitzing K, Ploog K and Weimann G 1986 *Solid State Commun.* **58** 5

[10] Ashoori R C and Silsbee R H 1992 *Solid State Commun.* **81** 821
[11] Zheng H-Z, Song A, Yang F-H and Li Y-X 1994 *Phys. Rev.* B **49** 1802
[12] Takaoka S, Oto K, Kurimoto H, Murase K, Gamo K and Nishi S 1994 *Phys. Rev. Lett.* **72** 3080
[13] Eisenstein J P, Stormer H L, Narayanamurti V, Cho A Y, Gossard A C and Tu C W 1985 *Phys. Rev. Lett.* **55** 875
[14] Templeton I M 1988 *J. Appl. Phys.* **64** 3570
[15] Elliott M, M. Harris G M, Herrenden-Harker W G, Shepherd R, Jones G A C, Ritchie D A, Linfield E H and Grimshaw M 1994 *Proc. 4th Int. Conf. on the Formation of Semiconductor Interfaces (Jülich, 1993)* (Singapore: World Scientific)
[16] Ando T and Uemura Y 1974 *J. Phys. Soc. Japan* **36** 959
[17] Wegner F 1983 *Z. Phys.* B **51** 279
[18] Sa-yakanit V, Choosiri N and Glyde H R 1988 *Phys. Rev.* B **38** 1340
[19] Raikh M E and Shahbazyan T V 1993 *Phys. Rev.* B **47** 1522
[20] Xie X C, Li Q P and Das Sarma S 1990 *Phys. Rev.* **42** 7132
[21] Efros A L, Pikus F G and Burnett V G 1992 *Solid State Commun.* **84** 91
[22] Efros A L, Pikus F G and Burnett V G 1993 *Phys. Rev.* B **47** 2233
[23] Gerhardts R R and Gudmundsson V 1986 *Phys. Rev.* B **34** 2999
[24] Jones C L, Usher A, Elliott M, Herrenden-Harker W G, Potts A, Shepherd R, Cheng T S and Foxon C T 1995 *Solid State Commun.* **95** 409
[25] Shoenberg D 1984 *J. Low Temp. Phys.* **56** 417
[26] Hirakawa K and Sakaki H 1986 *Phys. Rev.* B **33** 8291